Detection and Characterization of the Intermediate on the Folding Pathway of Human α-Lactalbumin†

Makoto Nozaka, Kunihiro Kuwajima, Katsutoshi Nitta, and Shintaro Sugai*

ABSTRACT: To discuss the relation between the folding mechanism and the chemical structure of proteins, the reversible unfolding reactions of human α-lactalbumin by acidification and by guanidine hydrochloride at 25 °C are studied by means of circular dichroism, difference spectra and pH-jump measurements and are compared with those for bovine α-lactalbumin. As shown previously for bovine α-lactalbumin, the folding process at neutral pH is not explained by a simple two-state mechanism but involves an intermediate form that has the same amount of helical structures as the native form. The transition between the intermediate and the fully denatured states is too rapid to be measured and corresponds to the helix–coil transition of the backbone. One of the differences of human α-lactalbumin from the bovine protein is the remarkable stability of the intermediate at neutral pH, which can be explained by differences in the primary chemical structure. Another difference is the existence at acid pH of an additional helical form, which is more helical than the native form. The transition from this to the intermediate or to the fully denatured one also is shown to resemble the helix–coil transition. The following folding scheme of human α-lactalbumin is proposed:

$$A_m \leftrightarrow \cdots \leftrightarrow A_1 \leftrightarrow A_0 \leftrightarrow A_{-1} \leftrightarrow \cdots \leftrightarrow A_{-n}$$
$$\updownarrow$$
$$N$$

Here N is the native form, and the intermediate is a macroscopic state distributed around the state A_0 at neutral pH, while the distribution in the acid and fully denatured states shifts toward A_m and A_{-n}, respectively.

The final process in protein biosynthesis is the folding of the polypeptide chain into its three-dimensional structure, which has been considered to be determined predominantly by the amino acid sequence (Anfinsen and Scheraga, 1975). The process is assumed to occur in several steps (Tanaka and Scheraga, 1975; 1977a,b; Ptitsyn and Rashin, 1975; Finkelstein, 1977); some ordered backbone structures (such as α helices, extended chains, and chain reversals) are formed at first because of short-range interactions, contact regions are nucleated among the residues both in the ordered and in the unordered structures, and the association of such nucleated regions dictated by long-range interactions leads to the formation of the native tertiary structure.

An approach to understanding the folding process is to investigate the intermediates in structure between the native and the unfolded states (Baldwin, 1975). From studies on the equilibrium and kinetics of folding and unfolding, conformational intermediates have been detected in carbonic anhydrase (Wong and Tanford, 1973), penicillinase (Robson and Pain, 1976a,b), and ribonuclease (Baldwin, 1975; Hagerman and Baldwin, 1976). The folding intermediates of carbonic anhydrase and penicillinase have secondary structures similar to those in the native state, although aromatic side chains are not found to pack into the globular hydrophobic regions. Such intermediates, however, have not yet been characterized sufficiently for discussion of the intimate relation between the stereoregular and the chemical structures.

In a series of papers from our laboratory, we have shown the existence of a stable intermediate on the folding pathway of BLA[1] (Nitta and Sugai, 1972; Sugai et al., 1973; Kuwajima et al., 1975, 1976; Kita et al., 1976; Okuda and Sugai, 1977; Nitta et al., 1977a,b; Kuwajima, 1977) and have characterized it by a variety of methods. The intermediate has been found to be similar to the acid-denatured form, which is also similar to the intermediate forms of carbonic anhydrase and penicillinase. One of us has proposed a folding model of BLA from a standpoint of the three-state mechanism (the native, the acid, and the fully denatured states) (Kuwajima, 1977). In this study, the intermediate on the folding pathway of HLA was found and characterized, and then the native structure of HLA and its folding process were discussed and compared with the folding process of BLA considering differences in the amino acid sequence between both the proteins.

Materials and Methods

Materials. α-Lactalbumin used in this study was prepared from fresh human milk by the method described previously (Kuwajima et al., 1976). It was completely homogeneous in a disc-gel electrophoresis pattern. The features of CD spectra for the protein coincided well with those reported by Cowburn et al. (1972). Stock solutions of the protein were filtrated through a membrane filter with a pore diameter of 0.45 μm just before measurements. The protein concentration was determined by absorption measurement at 280 nm. The value of $E_{280\text{nm}}^{1\%,1\text{cm}}$ was estimated to be 18.4 by the micro-Kjeldahl method. Specially prepared reagent-grade GuHCl was purchased from Nakarai Chemicals Ltd., and its concentration, c_{GuHCl}, was determined from the refractive index at 589 nm (Nozaki, 1972).

Methods. Difference spectra, CD, and pH measurement procedures have been described previously (Sugai et al., 1973; Kuwajima et al., 1976; Kita et al., 1976). For kinetic measurements at 25.0 °C, a rapid reaction analyzer (Union, RA-1100) and a rapid CD spectrophotometer (Union, CD-1000) were used with a digital memory and a kinetic data processor as previously shown (Nitta et al., 1977a,b).

† From the Department of Polymer Science, Faculty of Science, Hokkaido University, Sapporo 060, Japan. *Received February 22, 1978.* This research was partly supported by grants from the Ministry of Education of Japan.

[1] Abbreviations used: GuHCl, guanidine hydrochloride; BLA, bovine α-lactalbumin; HLA, human α-lactalbumin; CD, circular dichroism.

0006-2960/78/0417-3753$01.00/0

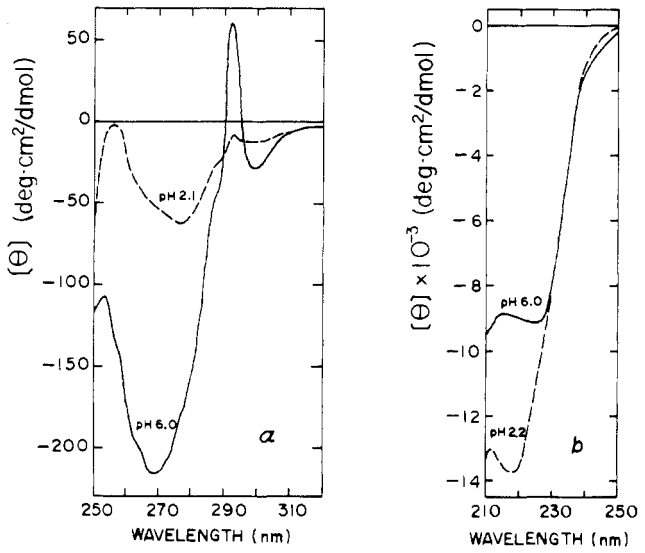

FIGURE 1: Circular dichroism spectra of HLA in the near- (a) and in the far- (b) ultraviolet regions at 25.0 °C. Solid lines represent the spectra in the native state: (a) 0 M GuHCl, pH 6.0; and (b) 1 M GuHCl, pH 6.0. Broken lines represent the spectra in the acid state: (a) 0 M GuHCl pH 2.1; and (b) 1 M GuHCl, pH 2.2. Protein concentrations are in the range of 0.05 to 0.1%. The path lengths of the optical cells used are 10 mm for the near-ultraviolet region and 0.2 mm for the far-ultraviolet region.

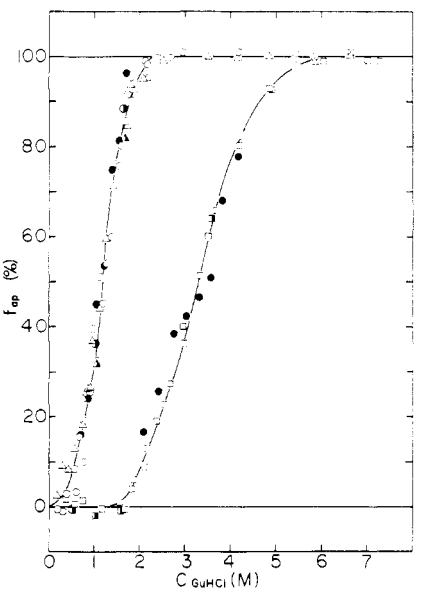

FIGURE 2: The dependence of f_{ap} on c_{GuHCl} at 25.0 °C. All solutions contain 0.01 M sodium phosphate (pH 6.0). The values of f_{ap} are calculated from the molar ellipticity at 270 nm, $[\theta]_{270}$ (○,◑), at 293 nm, $[\theta]_{293}$ (△,▲), and at 224 nm, $[\theta]_{224}$ (□,■), and from the difference extinction coefficient at 293 nm (cf. Figure 4) (●). Half-filled symbols refer to solutions prepared from protein originally in concentrated GuHCl and show reversibility of the transitions.

Results

To examine whether or not intermediates exist on the folding pathway of HLA, the reversible unfolding caused by treatments with acid and with GuHCl was followed by equilibrium and kinetic measurements.

Reversible Unfolding by Acid. The native HLA shows three CD bands in the near-ultraviolet region, at 270 (negative), 293 (positive), and 299 nm (negative) (Figure 1a), and all of them disappear almost completely at acid pH, although the ellipticity around 222 nm does not disappear on acidification (Figure 1b). Changes in the near-ultraviolet absorption spectrum were also observed during the acid transition of HLA, and the difference spectrum, characterized by three major extrema at 286 (blue shift), 293 (blue), and 301 nm (red), is similar to that for BLA. Therefore, as shown in the studies on the acid transition of BLA, the aromatic residues buried in the interior of the molecule appear to increase the rotational freedom during the transition (Kronman et al., 1965, 1972), although helical regions of the polypeptide chain remain undestroyed (Kuwajima et al., 1975, 1976).

Reversible Unfolding by GuHCl at Neutral pH. Figure 2 shows the apparent fractional extents of unfolding, f_{ap}, vs. c_{GuHCl} at pH 6.0 and 25.0 °C. Reversibility of the unfolding was confirmed by diluting samples in concentrated GuHCl with buffer solutions, and the values of f_{ap} were derived from the ellipticity changes at 270, 293, and 224 nm according to eq 1 in the previous paper (Kuwajima et al., 1976) with correction for solvent perturbation. The transitions observed at 270 and at 293 nm coincide well with each other, but the transition at 224 nm does not agree with these transitions. At 2 M GuHCl, the near-ultraviolet CD bands observed for the native HLA disappear almost completely, although the band around 222 nm does scarcely change in the region of c_{GuHCl} less than 2 M. These give clear evidence for the existence of at least one stable intermediate in the folding or unfolding process of HLA, and the structure of HLA at 2 M of the denaturant may be similar to its acid form.

Figure 3 shows the unfolding curve of HLA observed from the ultraviolet difference absorption at 293 nm. The unfolding

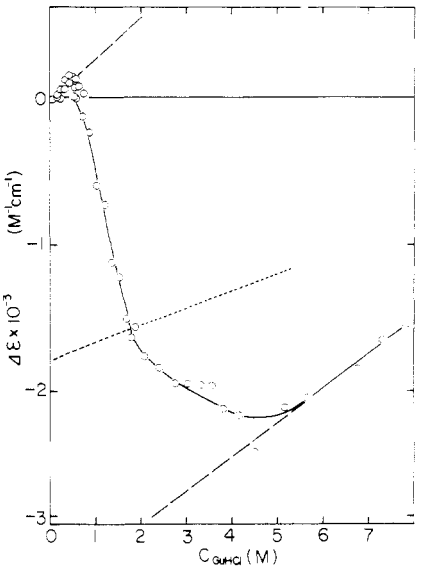

FIGURE 3: Difference molar extinction at 293 nm, $\Delta\epsilon_{293}$, as a function of c_{GuHCl} at pH 6.0 and 25.0 °C. Protein concentration is 0.0783%. Two broken lines refer to the hypothetical values of $\Delta\epsilon_{293}$ in the native and in the completely denatured states, respectively. The acid state is represented by a dotted line, which has been obtained experimentally by measuring the difference absorption at acid pH (pH ~1-2) and low concentrations of GuHCl.

occurs in two steps, and this is also a clear indication for the existence of at least one stable intermediate. The first step of the transition occurs in the range of c_{GuHCl} 0.5–2 M, which corresponds to the transition observed from CD ellipticity at 270 and at 293 nm, while the second step occurs in the range 2–5 M, which corresponds to the transition from ellipticity at 224 nm. If we assume the existence of one stable intermediate for which the solvent perturbation is the same as for the acid state (a dotted line in Figure 3), each transition observed from difference absorption coincides excellently with that from CD measurements (Figure 2).

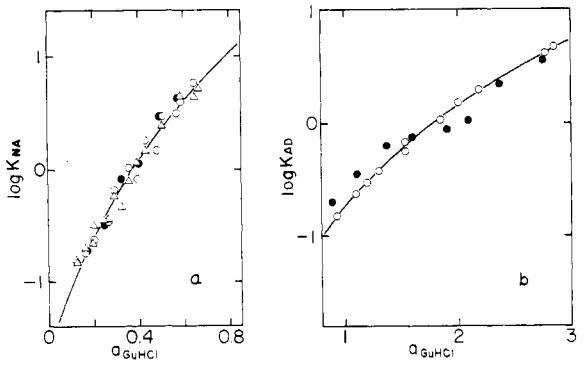

FIGURE 4: The dependence of the logarithmical equilibrium constants on a_{GuHCl}, calculated from the data in the transition region of each reaction in Figure 2: (a) log K_{NA} and (b) log K_{AD}. Open symbols refer to the values calculated from CD ellipticity: (a) $[\theta]_{270}$ (○), $[\theta]_{293}$ (△), and (b) $[\theta]_{224}$ (○). Filled circles refer to the values from $\Delta\epsilon_{293}$. Solid lines are theoretically calculated according to eq 2 by using the values in Table I. The values of f_{ap} (1st step) are regarded as unity at c_{GuHCl} higher than 2 M, and f_{ap} (2nd step) equals zero at c_{GuHCl} less than 2 M, in eq 1. Molar activity, a_{GuHCl}, was calculated from c_{GuHCl} as described by Aune and Tanford (1969).

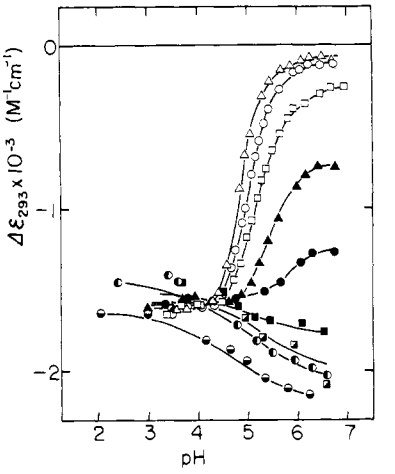

FIGURE 5: The variation of $\Delta\epsilon_{293}$ with pH at various fixed concentrations of GuHCl (25.0 °C): 0.6 (△), 0.8 (○), 1.0 (□), 1.25 (▲), 1.6 (●), 2.0 (■), 2.5 (◪), 3.1 (◐), and 4.0 M (◒). The reference solution is at pH 6.0 and 0 M GuHCl. All solutions contain 0.1 M CH_3COOK-CH_3COOH.

Thermodynamic Parameters of the Transitions. From the results above, a three-state mechanism in which the intermediate A is identical with the acid state can be assumed, as a first approximation, for the folding and unfolding of HLA:

$$N \rightleftharpoons A \rightleftharpoons D$$

where N and D mean the native and the completely unfolded states, respectively. The equilibrium constants of the transitions can be calculated from the fractions (f_N, f_A, and f_D) of the three states, where the fractions are given by

$$\begin{cases} f_N = 1 - f_{ap}\,(1\text{st step}) \\ f_A = f_{ap}\,(1\text{st step}) - f_{ap}\,(2\text{nd step}) \\ f_D = f_{ap}\,(2\text{nd step}) \end{cases} \quad (1)$$

If each transaction is due to the binding of GuHCl, the equilibrium constant of the transition from the i to j state, K_{ij} (= f_j/f_i), is expressed in terms of the conformational free energy in the absence of GuHCl, $\Delta G_{ij}^{H_2O}$, and of the change in the number of GuHCl binding sites during the transition, Δn_{ij}, as follows (Tanford, 1968, 1970):

$$\ln K_{ij} = -\Delta G_{ij}^{H_2O}/RT + \Delta n_{ij} \times \ln (1 + k a_{GuHCl}) \quad (2)$$

where a_{GuHCl} is the GuHCl activity, k is the binding constant of GuHCl to the protein and is assumed to be 3.00, and i or j means N, A, or D. In Figure 4a-b, log K_{NA} and log K_{AD} are plotted against a_{GuHCl}. The theoretical curve of the best fit to the data gives $\Delta G_{ij}^{H_2O}$ and Δn_{ij} (Table I).

Characterization of the N ⇌ A Transition. To determine more precisely the effect of pH on the transitions of HLA, we studied in detail the shifts in the difference extinction coefficient at 293 nm, $\Delta\epsilon_{293}$, and in the ellipticity at 270 nm, $[\theta]_{270}$, of HLA brought about by changing the pH at several fixed concentrations of GuHCl in the range 0.6-4.0 M. The data of $\Delta\epsilon_{293}$ are summarized in Figure 5. The molecule is in the N state at pH 6.0 at c_{GuHCl} <0.6 M, and in the A state at pH <4 in the range of c_{GuHCl} 0-2 M. The equilibrium constant K_{NA} can be evaluated from each point in Figure 5 in the range of c_{GuHCl} <2 M, where the transition seems to occur between the two states N and A. The values of log K_{NA} can be written as a sum of two functions; one depending on a_{GuHCl} alone (eq 2) and another on hydrogen ion activity alone (Tanford, 1970). Thus, as previously described (Kita et al., 1976), a master curve

TABLE I: Unfolding Parameters and Conformational Free Energy of HLA and BLA.[a]

	HLA			BLA[b]		
	N → A	A → D	N → D	N → A	A → D	N → D
$\Delta G_{ij}^{H_2O}$ (kcal/mol)	2.2	4.1	6.3	~4.1-4.4	2.5	6.5
Δn_{ij}	5.0	3.7	8.7	~4.9-5.3	3.0	7.9

[a] At pH ~6-7 and 25 °C. [b] Kita et al. (1976) and Kuwajima et al. (1976).

can be made for the pH dependence of the N ⇌ A transition. The resultant master curve is shown in Figure 6a, in which the data obtained from $[\theta]_{270}$ are also presented, and they are in good agreement with those from $\Delta\epsilon_{293}$.

On the other hand, the time courses of $\Delta\epsilon_{293}$ after the pH-jumps were measured under the condition of 2 < pH < 7 and 0.6 M < c_{GuHCl} < 1.6 M indicate that the transition appears to be a two-state reaction. The pH dependence of the apparent rate constant of the N ⇌ A transition was examined at 0.8 and 1.25 M GuHCl. The microscopic rate constants, k_f (forward) and k_r (reversed), can be obtained from the apparent rate constant k_{ap} (= $k_f + k_r$) and the equilibrium constant K_{NA} (= k_f/k_r). The master curves for the pH dependence of log k_f and log k_r can be made by the same method as reported previously (Kita et al., 1976), and these curves adjusted to 0.8 M GuHCl are shown in Figure 6b,c. The kinetics from rapid CD measurements at 270 nm were also examined, and the results are in good agreement with those from $\Delta\epsilon_{293}$. Three master curves in Figure 6 relate to the intrinsic dissociation constants, in the N, A*, and the A states, of the groups affecting the pH dependence of the N ⇌ A transition, where A* means the activated state along the transition pathway.

pH Dependence of the A ⇌ D Transition. The A ⇌ D transition occurs in the range of c_{GuHCl} higher than 2 M, where small changes in $\Delta\epsilon_{293}$ are observed with the change in pH (Figure 5). A master curve for the pH dependence of log K_{AD} is shown in Figure 7. The transition can be interpreted in terms of five carboxyl residues of pK_A = 4.6 and pK_D = 4.4 (Kuwajima, 1977); K_A and K_D are the dissociation constants in the A and D states. From kinetic measurements for the A ⇌ D transition, however, no change in $\Delta\epsilon_{293}$ was observed because the transition is too fast to be measured by the stopped-flow

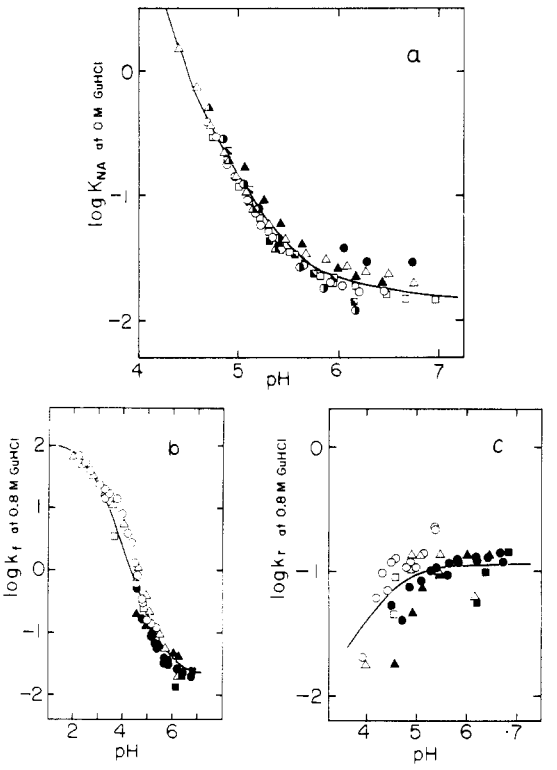

FIGURE 6: Master curves for the pH dependence of log K_{NA} (a), log k_f (b), and log k_r (c). The procedures for drawing the master curves have been described in detail by Kita et al. (1976). (a) The same symbols as in Figure 5 show the same experimental conditions. Three other symbols represent the values from the pH dependence of $[\theta]_{270}$ at c_{GuHCl}: 0.6 (▲), 0.8 (◑), and 1.0 M (■). The data have been adjusted to 0 M GuHCl using the parameter Δn_{NA} in Table I and eq 2. (b,c) Circles and triangles represent the values from the fast absorption measurements at 293 nm at 0.8 and 1.25 M GuHCl, respectively. Squares represent those from fast CD measurements at 270 nm at 0.8 M GuHCl. Open symbols denote the results of forward pH-jump directed from higher to lower pH values, while filled symbols represent the backward pH-jump. The data at 1.25 M GuHCl have been adjusted to 0.8 M GuHCl.

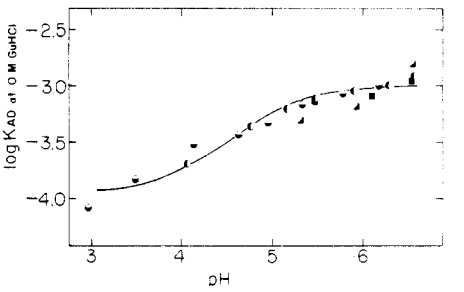

FIGURE 7: A master curve for the pH dependence of the A ⇌ D transition. Symbols are the same as in Figure 5. The solid curve is theoretically calculated in terms of the five Glu residues (shown in text) according to eq 24 in Tanford (1970).

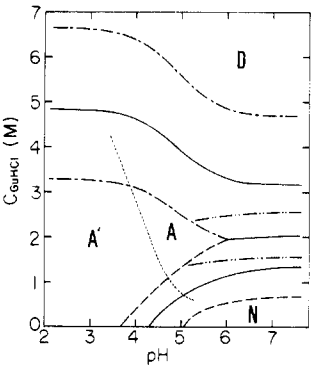

FIGURE 8: Phase diagram for the conformational states of HLA, in a solution of GuHCl, at any concentration and pH, at 25 °C. The solid lines represent the pH and GuHCl concentration where K_{NA}, K_{AD}, and K_{ND} ($= K_{NA}K_{AD}$) are equal to unity. The other lines, except for a dotted line, represent the pH and GuHCl concentration, where K_{NA} = 10, 0.1 (- - -), K_{AD} = 10, 0.1 (- · - · -) and K_{ND} = 10, 0.1 (-···-···-). The dotted line denotes the transition points of the A ⇌ A′ transition.

method, and then the relaxation time is estimated to be less than 1 ms considering the dead time of the apparatus.

Discussion

The folding process of HLA is very similar to that of BLA. It cannot be explained by the simple two-state mechanism. The intermediate can be assumed to be the acid form, as reported previously in the studies on BLA. Table I shows the thermodynamic parameters for each transition under the assumption of the three-state mechanism. The free energy of stabilization of the N state, $\Delta G_{ND}^{H_2O}$, is close to that of BLA. The present results are also consistent with a model for the folding of BLA postulated previously (Kuwajima, 1977); at the first step of folding, the fully denatured molecule forms helical structures dictated by local interactions (D → A), and then the hydrophobic interactions may make the packing of the helical segments (A → A*), which is followed by the final stabilization by the specific electrostatic interactions such as charge pair formation (A* → N).

However, some differences are found in the folding behavior and the intermediate structure between the two proteins. A difference can be seen in the plots of $\Delta\epsilon_{293}$ vs. c_{GuHCl} and of f_{ap} vs. c_{GuHCl} at neutral pH [Figures 3 and 2 (HLA), Figure 1 in Sugai et al. (1973), and Figure 2 in Kuwajima et al. (1976) (BLA)]. From these plots, the intermediate of HLA is found to be more stable than that of BLA. Remarkable stability of the A form of HLA is also supported by comparing the phase diagram for HLA (Figure 8) with that for BLA (Kuwajima et al., 1976).

Another essential difference between the proteins is the change in ellipticity around 222 nm on acidification at zero or at a low concentration of GuHCl. The ellipticity values of BLA do scarcely change (Kuwajima et al., 1976) but those of HLA decrease significantly (about 30%), indicating a significant increase in helical structures (Figure 1). The pH dependence of $[\theta]_{224}$ does not agree with that of $\Delta\epsilon_{293}$ in the acid region, as shown in Figure 9, which demonstrates that the acid transition of HLA at a low concentration of GuHCl is not truly a two-state reaction. Then, as a second approximation, we assume the following three-state mechanism for the acid transition (i.e., as a whole, a four-state mechanism among N, A′, A, and D):

$$N \underset{k_r^t}{\overset{k_f^t}{\rightleftharpoons}} A \underset{k_r'}{\overset{k_f'}{\rightleftharpoons}} A'$$

where A′ is an additional partially unfolded form, which is more stable at acid pH and more helical than the A form but cannot be distinguished from A only by $\Delta\epsilon_{293}$ measurements. Since all the time courses of the acid transition strictly obey first-order kinetics as observed for a two-state reaction, the A ⇌ A′ transition is due to the very fast change in the helical fraction, which cannot be observed by the stopped-flow method.

Because of k_f^t, $k_r^t \ll k_f'$, k_r', the true parameters of the N ⇌ A transition, K_{NA}^t, k_f^t and k_r^t, can be evaluated from the previous apparent parameters, K_{NA}, k_f and k_r:

$$K_{NA}^t = \frac{k_f^t}{k_r^t},\ k_f^t = k_f \text{ and } k_r^t = k_r(1 + K_{AA'}) \qquad (3)$$

TABLE II: α-Helical Regions of HLA and BLA Based on the Theoretical Predictions.[a]

	method	predicted α-helical regions
BLA	Chou and Fasman	7-13, 37-43, 104-110
	Robson and Suzuki	1-15, 111-123
	Lim	5-16, 77-89, 91-99, 105-110, 111-123
HLA	Chou and Fasman	7-13, 104-123
	Robson and Suzuki	4-11, 23-29, 86-95, 101-123
	Lim	7-15, 25-32, 77-89, 91-99, 105-110, 111-123

[a] Both BLA and HLA contain 123 amino acid residues, and their amino acid sequence data are taken from Brew et al. (1970) and Findlay and Brew (1972).

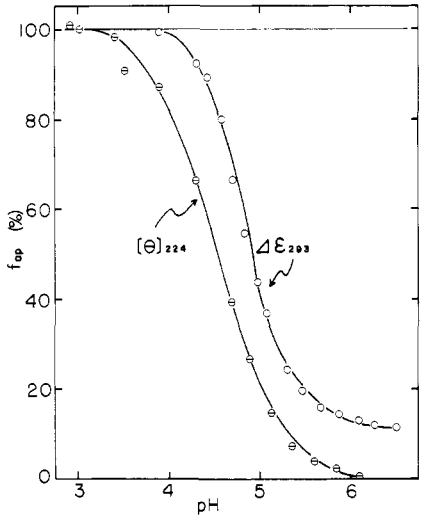

FIGURE 9: Acid transition curves of HLA at 0.6 M GuHCl and 25.0 °C by following the changes in difference extinction at 293 nm (O) and in CD ellipticity at 224 nm (Θ). The transitions are represented as the variations in apparent fractional extent, f_{ap}, with pH.

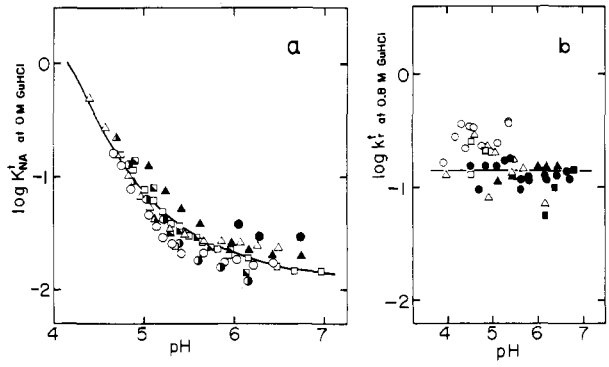

FIGURE 10: Corrected master curves for the pH dependence of log K_{NA}^t (a) and log k_r^t (b). Symbols are the same as in Figure 6. Solid curves in a and b and in Figure 6b are theoretically calculated with the following ionizable groups according to eq 24 in Tanford (1970); 1 carboxyl residue (pK_N = 2.4; pK_{A^*} = pK_A = 3.3), 1 carboxyl residue (pK_N = 3.9; pK_{A^*} = pK_A = 4.4), 5 carboxyl residue (pK_N = 4.2; pK_{A^*} = pK_A = 4.6), and 1 histidyl residue (pK_N = 5.8; pK_{A^*} = pK_A = 6.1), where K_N, K_{A^*} and K_A are the dissociation constants of the ionizable groups in the N, A*, and A states, respectively.

where $K_{AA'}$ (= k_f'/k_r') is the equilibrium constant of the A ⇌ A′ transition. The values of K_{NA}^t and k_r^t are plotted against pH in Figure 10, where k_r^t is almost independent of pH. The intrinsic dissociation constants in the N, A*, and A states of the groups affecting the pH dependence of the N ⇌ A transition can be obtained from Figures 6b and 10a,b. The electrostatic interactions such as charge pair formation are shown to be important at the final stage of the folding process (A* → N).

Recently, many workers have attempted to predict the local secondary structures in the native proteins (Tanaka and Scheraga, 1976; Chou and Fasman, 1974; Robson and Suzuki, 1976). Here we estimated the α-helical regions in HLA and in BLA by the methods of Chou and Fasman (1974) and of Robson and Suzuki (1976), and the results are compared with Lim's prediction data (Lim, 1974) in Table II, from which we can conclude that probable helical regions in the N state are 6-15, 105-110, and 111-123 for BLA and 7-13, 25-29, 86-89, 91-95, and 104-123 for HLA. The helical contents from the theoretical prediction are 0.24 (BLA) and 0.33 (HLA), which are in agreement with those [0.19 (BLA) and 0.22 (HLA)] from the CD data of both the proteins (Kuwajima et al., 1976; Cowburn et al., 1972) calculated by the Greenfield-Fasman method (1969). In the above helical regions of HLA, 18 of the strong helix-forming residues (Ala, Leu, and Glu) (Chou and Fasman, 1974) are found, while only 13 of them are found in the helical regions of BLA. The difference in stability of the A form observed between BLA and HLA may reflect the number of the strong helix-forming residues between the proteins. Also, in the helical regions of HLA are found five carboxyl residues, and all of them are glutamyl residues that seem to affect the pH dependence of the A ⇌ D transition (Kuwajima, 1977).

Finally, we should make one important comment for the folding scheme of HLA. Both the A ⇌ D and the A ⇌ A′ transitions are due to the very fast backbone conformational changes between the helical and coiled states, and they seem to be dictated predominantly by short-range interactions (Kuwajima, 1977). Then these transitions should be treated as a one-dimensional helix to coil system. Although we approximated the A′ ⇌ D transition to be of the three-state type with the intermediate A, the transition should rather be expressed by a multidistributed or continuously distributed state type. Therefore, the folding scheme of HLA (Scheme I) is proposed. The A state described previously is a macroscopic state statistically distributed around the microscopic state A_0 at neutral pH, while the distribution in the A′ and D states

Scheme I

$$A_m \rightleftharpoons A_{m-1} \rightleftharpoons \cdots \rightleftharpoons A_1 \rightleftharpoons A_0 \rightleftharpoons A_{-1} \rightleftharpoons \cdots \rightleftharpoons A_{-(n-1)} \rightleftharpoons A_{-n}$$

$$\Updownarrow$$

$$N$$

shifts toward A_m and A_{-n}, respectively. Justification of such a folding mechanism will be made clear by advanced studies.

Acknowledgments

The interpretation of the data is the result of many helpful discussions with Professor Michio Yoneyama to whom the authors are very grateful.

References

Anfinsen, C. B., and Scheraga, H. A. (1975), *Adv. Protein Chem. 29,* 205.
Aune, K. C., and Tanford, C. (1969), *Biochemistry 8,* 4586.
Baldwin, R. L. (1975), *Annu. Rev. Biochem. 44,* 453.
Brew, K., Castellino, F. J., Vanaman, T. C., and Hill, R. L. (1970), *J. Biol. Chem. 245,* 4570.
Chou, P. Y., and Fasman, G. D. (1974), *Biochemistry 13,* 222.
Cowburn, D. A., Brew, K., and Gratzer, W. B. (1972), *Biochemistry 11,* 1228.
Findlay, J. B. C., and Brew, K. (1972), *Eur. J. Biochem. 27,* 65.
Finkelstein, A. V. (1977), *Biopolymers 16,* 525.
Greenfield, N., and Fasman, G. D. (1969), *Biochemistry 8,* 4108.
Hagerman, P. J., and Baldwin, R. L. (1976), *Biochemistry 15,* 1462.
Kita, N., Kuwajima, K., Nitta, K., and Sugai, S. (1976), *Biochim. Biophys. Acta 427,* 350.
Kronman, M. J., Cerankowski, L., and Holmes, L. G. (1965), *Biochemistry 4,* 518.
Kronman, M. J., Jeroszko, J., and Sage, G. W. (1972), *Biochim. Biophys. Acta 285,* 145.
Kuwajima, K. (1977), *J. Mol. Biol. 114,* 241.
Kuwajima, K., Nitta, K., and Sugai, S. (1975), *J. Biochem. (Tokyo) 78,* 205.
Kuwajima, K., Nitta, K., Yoneyama, M., and Sugai, S. (1976), *J. Mol. Biol. 106,* 359.
Lim, V. I. (1974), *J. Mol. Biol. 88,* 873.
Nitta, K., and Sugai, S. (1972), *Biopolymers 11,* 1893.
Nitta, K., Kita, N., Kuwajima, K., and Sugai, S. (1977a), *Biochim. Biophys. Acta 490,* 200.
Nitta, K., Segawa, T., Kuwajima, K., and Sugai, S. (1977b), *Biopolymers 16,* 703.
Nozaki, Y. (1972), *Methods Enzymol. 26,* 43.
Okuda, T., and Sugai, S. (1977), *J. Biochem. (Tokyo) 81,* 1051.
Ptitsyn, O. B., and Rashin, A. A. (1975), *Biophys. Chem. 3,* 1.
Robson, B., and Pain, R. H. (1976a), *Biochem. J. 155,* 325.
Robson, B., and Pain, R. H. (1976b), *Biochem. J. 155,* 331.
Robson, B., and Suzuki, E. (1976), *J. Mol. Biol. 107,* 327.
Sugai, S., Yashiro, H., and Nitta, K. (1973), *Biochim. Biophys. Acta 328,* 35.
Tanaka, S., and Scheraga, H. A. (1975), *Proc. Natl. Acad. Sci. U.S.A. 72,* 3802.
Tanaka, S., and Scheraga, H. A. (1976), *Macromolecules 9,* 168.
Tanaka, S., and Scheraga, H. A. (1977a), *Proc. Natl. Acad. Sci. U.S.A. 74,* 1320.
Tanaka, S., and Scheraga, H. A. (1977b), *Macromolecules 10,* 291.
Tanford, C. (1968), *Adv. Protein Chem. 23,* 121.
Tanford, C. (1970), *Adv. Protein Chem. 24,* 1.
Wong, K., and Tanford, C. (1973), *J. Biol. Chem. 248,* 8518.